

Reference Shaping for Model-Based Control of Biomass Grate Boilers*

Richard Seeber^{a,*}, Markus Göllés^b, Nicolaos Dourdoumas^a, Martin Horn^{a,b}

^a*Institute of Automation and Control, Graz University of Technology, Graz, Austria*

^b*Bioenergy 2020+ GmbH, Graz, Austria*

Abstract

An established control strategy for biomass grate boilers based on a low-order nonlinear model is considered. Under ideal conditions, it achieves decoupled control of desired outputs by means of input-output linearization. The decoupling is gradually reduced and control performance deteriorates when actuator saturation occurs. This may be avoided by appropriately shaping the control strategy's reference values. This contribution presents a method to do so by solving a sequence of linear programs. Its implementation requires the knowledge of typically unknown limits of mass-flows fed into the plant. An estimation strategy for these limits based on measurable quantities is thus proposed. Experimental data from three different scenarios is presented, in which the reference shaping improves tracking, mitigates wind-up phenomena and reduces emissions, respectively.

Keywords: actuator saturation; reference shaping; command governor; reference governor; conditioning technique; model-based control; input-output linearization; biomass combustion

1. Introduction

In recent years, biomass has increased in importance as a solid fuel for combustion due to the goal of reducing carbon dioxide emissions. Controlling biomass boilers has thus become more important, with low emissions, high efficiency, good load modulation capability and high fuel flexibility being the main goals. Conventionally, PID controllers are used for this task, see e.g., van Loo and Koppejan (2008); Plaček et al. (2011); Kaltschmitt et al. (2016). As the plant is a nonlinear system with multiple inputs and outputs, the performance achievable this way is limited. This has prompted the development of models and model-based control strategies, which promise significant improvements in this regard. Several contributions consider experimentally obtained linear or linearized models, which are used as a basis for model predictive control schemes, e.g. Paces et al. (2011); Kortela and Jämsä-Jounela (2012).

Using physical principles, a low order nonlinear model is developed in Bauer et al. (2008, 2010). In Göllés et al.

(2011), a control strategy based on this model is proposed. It utilizes the input-output linearization technique along with an extended Kalman filter, see e.g. Isidori (1995); Daoutidis and Kravaris (1994), in order to decouple and linearize the plant dynamics, and PI-controllers to avoid steady-state control deviations. In the course of experiments, this strategy exhibited significant performance improvements over a conventional control scheme. Various improvements yielding further increases in performance are proposed in Seeber et al. (2014); Schörghuber et al. (2015). The strategy has since then successfully been used for long-term operation of an industrial-scale biomass boiler, see Zemann et al. (2014). A similar strategy has also been applied to a small-scale biomass boiler in Göllés et al. (2014).

An open problem of this strategy still occurs in the presence of actuator limitations. Typically, not all desired set-points are achievable within the available actuator range. While windup effects are mitigated to some extent by selectively stopping certain integrators, cross-couplings and nonlinearities are not fully compensated during actuator saturation. This deteriorates control performance in the form of increased undesirable variations of some controlled outputs. Additionally, the remaining windup effects may lead to overshoots when the operating point is changed. Depending on which outputs are affected, these output deviations may even lead to an increase in emissions or reduce the furnace's service life.

To reduce the integrator windup, more advanced anti-windup techniques may be used. There is a wide range of such techniques available for linear systems, see e.g., Åström and Rundqwist (1989); Kothare et al. (1994); Berger

*This work is the result of a cooperation between the Institute of Automation and Control, Graz University of Technology and the research center Bioenergy 2020+ GmbH. The research leading to these results has received funding from the COMET program managed by the Austrian Research Promotion Agency under grant number 844605. The program is co-financed by the Republic of Austria and the Federal Provinces of Burgenland, Lower Austria and Styria.

*Corresponding author

Email addresses: richard.seeber@tugraz.at (Richard Seeber), markus.goelles@bioenergy2020.eu (Markus Göllés), nicolaos.dourdoumas@tugraz.at (Nicolaos Dourdoumas), martin.horn@tugraz.at (Martin Horn)

and Gutman (2016), and also a few techniques that are applicable to input-affine nonlinear systems, such as Kendi and Doyle III (1997); Herrmann et al. (2010); Gomes da Silva Jr. et al. (2014), for example. Dealing with the windup on its own still would leave the problem of undesired output deviations unsolved, however. Therefore, the modification of references by means of a shaping filter is considered here. The necessity for such a reference modification in the context of the present application is already acknowledged in Gölles et al. (2011), where the use of expert rules is suggested for this purpose. These take only the most commonly occurring actuator limitations into account, however, and their design requires significant process insight. The present paper proposes a general technique for reference shaping that can deal with arbitrary combinations of actuator limitations.

In the context of windup prevention, the basic idea of a reference shaping filter is discussed in Hippe (2006). It may also be interpreted in the sense of the conditioning technique proposed in Hanus et al. (1987), which consists in feeding a modified reference to the integrators such that the control input never saturates. A closely connected concept are so-called reference governors and command governors, which also prevent actuator saturation by an appropriate modification of references. Their design is extensively studied in literature, see e.g., Garone et al. (2017) for a quite comprehensive overview. In Kapasouris et al. (1988), and later, e.g., in Gilbert et al. (1994); Bemporad et al. (1997), linear systems with constrained control inputs and states are considered. There, the references are modified by solving an optimization problem subject to the modified reference being contained in the so-called maximal constraint admissible set, see Gilbert and Tan (1991). Inside this set, the state and input constraints are guaranteed to be satisfied for all future time instants with constant reference values. For nonlinear systems, this idea is applied for example in Vahidi et al. (2007) by considering a linearized version of the system and treating the difference between the linear and the nonlinear behavior as a disturbance. Approaches that use the full nonlinear or a feedback-linearized model also exist, see e.g., Bemporad (1998); Kalabić et al. (2011). The optimization problems obtained in this case are usually non-convex, however, and finding their global optimum is challenging, especially when multiple references are considered.

The reference shaping strategy proposed in the present contribution follows an approach similar to the optimization based command governors. Unlike these, however, it does not consider maximal constraint admissible sets. This is due to the fact that considering them would only provide guarantees for constant references and disturbances, which may vary (sometimes unpredictably), however. Furthermore, computing them is also rather complicated due to the nonlinear nature of the plant. Considering possible future variations of the disturbances, as it is done for linear systems in Kolmanovsky and Gilbert (1998), for example, would increase the complexity even further. Therefore,

the control inputs are instead constrained to the admissible actuator range at each time step. This does not permit to directly enforce constraints for the outputs, which are required to ensure the safe operation of the plant; instead, constraints for the shaped references are considered. While this does not guarantee that the outputs satisfy the same constraints at all times, it is still effective in limiting the outputs to values that ensure a safe operation of the plant.

The optimization procedure used by the reference shaping strategy is based on a sequential optimization. This is similar to the concept employed by the Prioritized Reference Governor, which is proposed for linear time-invariant systems in Kalabić et al. (2013). Sequential optimization has also successfully been applied in other contexts, such as biomedical engineering and robotics, where it is used to deal with multiple goals that have different priorities, see e.g. De Lasa and Hertzmann (2009); Falkinger et al. (2012). Here, the sequential approach guarantees that control deviations of certain, low-priority outputs are preferred in favor of violating higher priority goals, such as that of providing the desired power output, while at the same time avoiding actuator saturations. It is shown that despite the nonlinear plant the optimization problems resulting from this general strategy can be reduced to a sequence of linear programs. These convex optimization problems can be solved efficiently and make the approach attractive also from a computational point of view.

The technique is applicable to a big variety of biomass grate boilers or to any plant with a similarly structured mathematical model. It is discussed in this paper using the model and control strategy described in Gölles et al. (2011) with the improvements from Seeber et al. (2014) as a basis. In the course of experiments, it is then applied to a representative medium-scale biomass grate boiler. It is shown that the proposed reference shaping improves the control performance when actuator constraints are active by reducing undesired variations of controlled outputs to a minimum. Additionally, windup effects are effectively mitigated, because the actuators never exceed the limits with the modified references.

The paper is structured as follows: Section 2 gives an overview of a typical biomass grate boiler's operation. Section 3 summarizes the existing model and control strategy that motivate the work presented in this paper. In Section 4 the reference shaping strategy is proposed assuming a fairly general nonlinear model structure. Section 5 discusses issues of applying this strategy to the particular plant model and control strategy at hand. Experimental results comparing the control concept with and without reference shaping, that are obtained on the plant at hand, are presented in Section 6. Section 7 concludes the paper.

2. Principle of Biomass Grate Boiler Operation

Fig. 1 shows a schematic overview of a typical biomass boiler for grate combustion of solid biomass fuels. Spa-

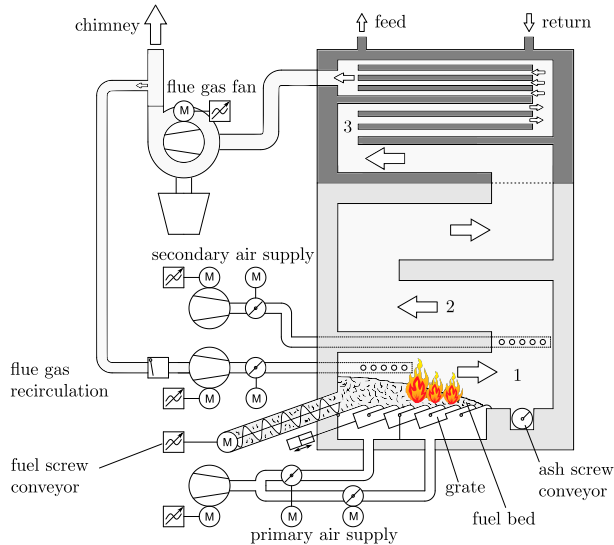


Figure 1: Schematic overview of a typical biomass grate boiler (1 ... primary combustion zone, 2 ... secondary combustion zone, 3 ... heat exchanger) Schörghuber et al. (2015)

tially, it is sub-divided into three areas: primary combustion zone, secondary combustion zone and heat exchanger.

A fuel screw conveyor transports biomass fuel (wood chips) into the combustion chamber. There the biomass is heated, which leads to the evaporation of the water it contains. Combustion of the dry fuel then takes place with the primary air fed in from below the grate. A fan and control valves are used to control this air mass-flow. Typically only part of the air required for complete combustion is supplied as primary air, leading to a partial combustion at this point. Secondary air is thus injected at high velocities at the end of the primary combustion zone. This leads to a complete combustion of the flue gas in the secondary combustion chamber. In order to influence the combustion temperature, in addition to the air a part of the (comparatively cold) flue gas from the chimney is recirculated into the combustion chamber.

The hot flue gas travels through the heat exchanger, where part of its thermal energy is transferred to a water mass-flow; the water enters the heat exchanger in the form of cold return water and is heated by the flue gas, leaving the heat exchanger as hot feed water.

Finally, the flue gas leaves the plant through the chimney, with part of it being recirculated as mentioned before. A flue gas fan ensures a constant sub-atmospheric pressure inside the furnace to prevent any flue gas from escaping.

3. Existing Plant Model and Control Strategy

This section outlines the existing plant model as developed in Bauer et al. (2008); Göllés et al. (2011); Bauer et al. (2010) and the existing control strategy described in Seeber et al. (2014), which evolved out of Göllés et al. (2011) and forms the basis for the proposed reference shaping strategy.

The grate boiler's dynamics are modeled by a nonlinear fourth order model, with a third order model being used for control design. This latter model neglects the dynamics of one very slowly varying state variable (the furnace refractory lining's mean temperature), which is considered as an approximately constant disturbance instead.

Using this model, an input-output linearization control law is designed. An unstable internal dynamics resulting from this technique is stabilized by means of a P-controller that prescribes the amount of fuel fed into the plant. Additionally, PI-controllers are applied to the linearized and decoupled plant in order to improve the rejection of disturbances

State variables and disturbances required by the input-output linearization are estimated using an extended Kalman filter. Its particular structure is of no consequence for the remainder of the paper, and is thus not described here; for details in that regard the reader is referred to Seeber et al. (2014).

3.1. Nonlinear Mathematical Model

Manipulated physical inputs are the mass-flows of dry fuel, primary air, secondary air and recirculated flue gas. They are denoted by \dot{m}_{ff} , \dot{m}_{pa} , \dot{m}_{sa} and \dot{m}_{rf} , respectively. (A list of symbols along with their meaning is given in the appendix.) In addition, a number of disturbances act on the plant; these will be introduced as required during the presentation of the model.

The model consists of three parts: fuel bed, gas phase combustion and heat-exchanger. For the *fuel bed* a second order model as proposed in Bauer et al. (2010) is used. The state variables are masses of water and dry fuel in the fuel bed, denoted by m_w and m_f , respectively. The model is obtained from mass balance equations and can be written as

$$\frac{dm_w}{dt} = \frac{-\dot{m}_{\text{wev}} + w_f \dot{m}_{\text{ff}}(t - t_{\text{df}})}{1 + C_4 w_f} \quad (1a)$$

$$\frac{dm_f}{dt} = -\dot{m}_{\text{thd}} + \frac{C_4 \dot{m}_{\text{wev}} + \dot{m}_{\text{ff}}(t - t_{\text{df}})}{1 + C_4 w_f}. \quad (1b)$$

with the water content w_f of the biomass based on the *dry* fuel mass acting as a disturbance, and t_{df} being a delay caused by the aforementioned heating phase before combustion. The quantities \dot{m}_{wev} and \dot{m}_{thd} denote the mass-flows of evaporated water and thermally decomposed fuel, respectively, and are given by

$$\dot{m}_{\text{wev}} = C_1 m_w, \quad \dot{m}_{\text{thd}} = C_2 \alpha_{\text{th}} m_f \cdot [\dot{m}_{\text{pa}} + C_3]. \quad (2)$$

Therein C_1, \dots, C_4 are constant model parameters obtained from measurement data, and the disturbance α_{th} is a periodically time-varying fuel decomposition factor whose time-average is one. The denominator term $1 + C_4 w_f$ in (1) occurs due to the interaction of the water content and the delay caused by heating the fuel; see Bauer et al. (2010) for details in that regard.

The *combustion* model relates the mass-flows \dot{m}_{wev} and \dot{m}_{thd} as well as the air and recirculated flue gas mass-flows fed into the plant with the resulting flue-gas' mass flow \dot{m}_{fg} , oxygen content ν_{ox} and temperature T_{fg} by means of a combustion calculation, see e.g. van Loo and Koppejan (2008). This is a static relation obtained from mass and energy balance equations, and is common in the thermodynamic modelling of combustion processes. To illustrate the basic structure of these relations, the vector

$$\dot{\mathbf{m}}_{\text{c}} := [\dot{m}_{\text{pa}} + \dot{m}_{\text{sa}} + \dot{m}_{\text{fa}} \quad \dot{m}_{\text{rf}} \quad \dot{m}_{\text{wev}} \quad \dot{m}_{\text{thd}}]^{\text{T}} \quad (3)$$

containing all mass-flows contributing to the flue gas is introduced. It contains, in addition to the mass-flows already mentioned, also the false air \dot{m}_{fa} which enters the combustion chamber in addition to the primary and secondary air and acts as a disturbance. The combustion model can be written as

$$\dot{m}_{\text{fg}} = \mathbf{1}^{\text{T}} \dot{\mathbf{m}}_{\text{c}}, \quad \nu_{\text{ox}} = \frac{\boldsymbol{\ell}_1^{\text{T}} \dot{\mathbf{m}}_{\text{c}}}{\boldsymbol{\ell}_2^{\text{T}} \dot{\mathbf{m}}_{\text{c}}}, \quad T_{\text{fg}} = \frac{\boldsymbol{\ell}_3^{\text{T}} \dot{\mathbf{m}}_{\text{c}}}{\dot{m}_{\text{fg}}}. \quad (4a)$$

Therein $\mathbf{1}$ denotes a vector of ones, and the vectors $\boldsymbol{\ell}_1, \boldsymbol{\ell}_2$ and $\boldsymbol{\ell}_3$ consist of model parameters that depend on physical constants and three disturbances: the mean temperature of the furnace's refractory lining T_{r1} and the specific enthalpies of air and recirculated flue gas. Also computed at this point is the air ratio in the fuel bed, which is designated by λ_{fb} and is of interest from a control point of view. This is the ratio of oxygen fed to the fuel bed to the minimum oxygen required for complete combustion. It is given by

$$\lambda_{\text{fb}} = C_5 \frac{\dot{m}_{\text{pa}}}{\dot{m}_{\text{thd}}} \quad (4b)$$

with a constant model parameter C_5 and under typical conditions is less than one.

The *heat-exchanger* is modeled as proposed in Bauer et al. (2008) by a first order system for the hot water feed temperature T_{f} given by

$$\frac{dT_{\text{f}}}{dt} = C_6 \dot{m}_{\text{fg}} T_{\text{fg}} + C_7 \dot{m}_{\text{w}} [T_{\text{r}}(t - t_{\text{dr}}) - T_{\text{f}}]. \quad (5)$$

Therein C_6 and C_7 are again constant model parameters. The water mass-flow \dot{m}_{w} through, as well as the return temperature T_{r} at the heat-exchanger act as disturbances, with the latter being delayed by a delay t_{dr} that depends on \dot{m}_{w} .

In the following, the state variables—the masses of fuel and water in the fuel bed, and the feed temperature—are collected in the vector

$$\mathbf{x} = [x_1 \quad x_2 \quad x_3]^{\text{T}} := [m_{\text{w}} \quad m_{\text{f}} \quad T_{\text{f}}]^{\text{T}}. \quad (6)$$

The mass-flows fed into the plant are aggregated in the control input vector \mathbf{u} in the form

$$\mathbf{u} := \begin{bmatrix} u_1 \\ u_2 \\ u_3 \\ u_4 \end{bmatrix} = \begin{bmatrix} \dot{m}_{\text{ff}} \\ \dot{m}_{\text{pa}} + C_3 \\ \dot{m}_{\text{rf}} \\ \dot{m}_{\text{pa}} + \dot{m}_{\text{sa}} \end{bmatrix}. \quad (7)$$

This is done to simplify a few expressions in the model, such as e.g. the mass flows from (2) to

$$\dot{m}_{\text{wev}} = C_1 x_1, \quad \dot{m}_{\text{thd}} = \alpha_{\text{th}} C_2 x_2 u_2. \quad (8)$$

Variables to be controlled are the flue-gas' oxygen content $\nu_{\text{ox}} =: y_1$, the flue-gas temperature at the inlet of the heat exchanger $T_{\text{fg}} =: y_2$, the feed temperature $T_{\text{f}} =: y_3$ and the air-ratio in the fuel bed $\lambda_{\text{fb}} =: y_4$.

All disturbances are aggregated in a vector \mathbf{d} , whose particular structure is of no importance. The overall plant dynamics can then be expressed as

$$\frac{d\mathbf{x}}{dt} = \mathbf{f}(\mathbf{x}, \mathbf{u}, \mathbf{d}) \quad (9)$$

with a nonlinear function \mathbf{f} obtained from the interconnection of the presented models; see Gölles et al. (2011) for more details in that regard.

3.2. Input-Output Linearization

The inputs u_2, u_3 and u_4 are used to control the first three outputs $[y_1 \quad y_2 \quad y_3]^{\text{T}} =: \mathbf{y}$ by means of the input-output linearization technique, see e.g., Isidori (1995). The first input u_1 can not be used in this way due to the fact that it affects the model only after the significant dead-time t_{dr} . Thus, it is not considered here, but will be used in the following section to stabilize an internal dynamics, which arises in the course of the input-output linearization, by means of a P-controller.

The vector relative degree of the system is $d = (0, 0, 1)$. Thus, one wants the closed loop to be governed by the differential equations

$$y_1 = v_1, \quad (10a)$$

$$y_2 = v_2, \quad (10b)$$

$$\tau \frac{dy_3}{dt} + y_3 = v_3 \quad (10c)$$

with new inputs $[v_1 \quad v_2 \quad v_3]^{\text{T}} =: \mathbf{v}$ and a constant positive parameter τ . These three equations do not depend on u_1 but uniquely determine the remaining three control inputs. From (4a) and (5) one can see using (3) and (7) that each of the equations in (10) can be written in the form

$$v_i = \frac{\mathbf{a}_{e,i}^{\text{T}} \mathbf{u} + b_{e,i}}{\mathbf{c}_{e,i}^{\text{T}} \mathbf{u} + d_{e,i}} \quad \text{for } i = 1, 2, 3 \quad (11)$$

with suitable vectors $\mathbf{a}_{e,i}, \mathbf{c}_{e,i}$ and scalars $b_{e,i}, d_{e,i}$ depending on the state \mathbf{x} , the disturbance \mathbf{d} and the model parameters. The denominator of these expressions is assumed to be positive for physically meaningful values of \mathbf{u} . This is not a restriction, because a sign change of the denominator would lead to infinite, and hence physically impossible, plant outputs. The input-output linearization state-feedback control-law is obtained as the solution of these three equations with respect to u_2, u_3 and u_4 .

The input-output linearization leads to an unstable internal dynamics of order two. In Schörghuber et al. (2015) this internal dynamics is computed and investigated in more detail; here it is sufficient to know that the lack of stability is caused by the fuel mass m_f exhibiting integrator dynamics. This can most easily be seen from a physical point of view: if the power output of the plant is kept constant and no fuel is fed into the plant, the energy present in the form of dry fuel in the fuel bed reduces at a constant rate.

3.3. Fuel-Feed Controller

To stabilize the fuel mass $m_f = x_2$, the remaining input is used: the fuel mass-flow u_1 . Considering the significant dead time pertaining to u_1 this is done by means of a P-controller

$$u_1 = k_P(x_{s,2} - x_2) + u_{s,1} \quad (12)$$

with a set-point $x_{s,2}$ and an additional feed-forward part $u_{s,1}$ whose computation is discussed below, and a constant positive parameter k_P . The choice of k_P as well as a more sophisticated control strategy that is not used here are discussed in Schörghuber et al. (2015).

The feed-forward part corresponds to the steady-state fuel-feed required to maintain the set-point. Both quantities $u_{s,1}$ and $x_{s,2}$ are computed using a steady-state computation for the model (1)–(5) with outputs y_1, \dots, y_4 equal to given *desired* references $[r_{d,1} \ r_{d,2} \ r_{d,3} \ r_{d,4}] =: \mathbf{r}_d$, and the fuel decomposition factor α_{th} set to its mean value, one. The latter are *not* denoted \mathbf{r} to avoid confusion when discussing reference shaping later on. Setting the derivatives to zero in (1) yields the equation $\dot{m}_{ff} = \dot{m}_{thd}$. Using (7) and (8) one thus obtains the equilibrium of the fuel mass m_f as

$$x_{s,2} = \frac{u_{s,1}}{C_{22}u_{s,2}} \quad (13)$$

with $u_{s,2}$ denoting the steady-state¹ value of u_2 . Combination with (4) furthermore yields, after some calculations, equations similar to (11) characterizing the steady-state inputs \mathbf{u}_s

$$r_{d,i} = \frac{\mathbf{a}_{s,i}^T \mathbf{u}_s + b_{s,i}}{\mathbf{c}_{s,i}^T \mathbf{u}_s + d_{s,i}} =: g_{s,i}(\mathbf{u}_s) \quad \text{for } i = 1, 2, 3, 4. \quad (14)$$

The right hand side is a vector valued function $\mathbf{g}_s(\mathbf{u}_s)$ whose coefficients $\mathbf{a}_{s,i}$, $b_{s,i}$, $\mathbf{c}_{s,i}$ and $d_{s,i}$ depend on the model parameters and the slowly varying disturbances contained in \mathbf{d} . Again, the denominators of these expressions are assumed to be positive for sensible values of \mathbf{u}_s .

¹Due to the periodically varying disturbance α_{th} , a *constant* steady state will never occur in practice. It will be shown (and taken into account), however, that in *periodic* steady-state operation, only u_2 exhibits periodic variations while all other plant inputs and states are constant.

3.4. PI-Controllers

When the input-output linearization is used on its own, unknown disturbances typically cause stationary deviations of the outputs y_i from the corresponding inputs v_i of the input-output linearization. To improve stationary behavior, v_i are determined by means of PI-controllers with a feed-forward path of the form

$$\frac{d\eta_i}{dt} = r_{d,i} - y_i \quad (15a)$$

$$v_i = r_{d,i} + K_{P,i}(r_{d,i} - y_i) + K_{I,i}\eta_i \quad (15b)$$

for $i = 1, 2, 3$. Therein $K_{P,i}$ and $K_{I,i}$ are constant, positive controller parameters and η_i are the integrator states.

In the following discussions the structure of (14), which relates the desired references and steady-state control inputs, will turn out to be useful; similarly structured equations are thus derived also for the combination of input-output linearization and PI-controllers. Combining (15b) with (11) yields the relations

$$\begin{aligned} r_{d,i} &= \frac{1}{1 + K_{P,i}} \left(K_{P,i}y_i - K_{I,i}\eta_i + \frac{\mathbf{a}_{e,i}^T \mathbf{u} + b_{e,i}}{\mathbf{c}_{e,i}^T \mathbf{u} + d_{e,i}} \right) \\ &= \frac{\mathbf{a}_{p,i}^T \mathbf{u} + b_{p,i}}{\mathbf{c}_{p,i}^T \mathbf{u} + d_{p,i}} =: g_{p,i}(\mathbf{u}) \quad \text{for } i = 1, 2, 3. \end{aligned} \quad (16a)$$

Those define a vector valued function $\mathbf{g}_p(\mathbf{u})$ whose coefficients are given by

$$\begin{aligned} \mathbf{a}_{p,i} &= \mathbf{a}_{e,i} + (K_{P,i}y_i - K_{I,i}\eta_i)\mathbf{c}_{e,i}; & \mathbf{c}_{p,i} &= (1 + K_{P,i})\mathbf{c}_{e,i} \\ b_{p,i} &= b_{e,i} + (K_{P,i}y_i - K_{I,i}\eta_i)d_{e,i}; & d_{p,i} &= (1 + K_{P,i})d_{e,i}. \end{aligned} \quad (16b)$$

In addition to \mathbf{x} , \mathbf{d} and the model parameters, these coefficients depend on the integrator states, the measured output values and the PI-controller parameters.

3.5. Actuator Limitations and Anti-Windup Strategy

Due to actuator limitations, the mass-flows are constrained to values between (nonnegative) minima and maxima. Defining vectors of mass-flows fed into the plant

$$\dot{\mathbf{m}} := [\dot{m}_{ff} \ \dot{m}_{pa} \ \dot{m}_{sa} \ \dot{m}_{rf}]^T \quad (17)$$

and of their respective minima and maxima, $\dot{\mathbf{m}}_{\min}$ and $\dot{\mathbf{m}}_{\max}$, the constraints are given by

$$\dot{\mathbf{m}}_{\min} \leq \dot{\mathbf{m}} \leq \dot{\mathbf{m}}_{\max}. \quad (18)$$

In the existing control strategy, the mass-flows computed by the control algorithm are constrained to attainable values by component-wise saturation functions. To avoid excessive integrator windup, a simple anti-windup strategy is employed that consists of stopping certain integrators on actuator saturation. The particular integrators to stop are selected based on process insight, see Gölle et al. (2011); for example, on saturation of \dot{m}_{rf} , whose main purpose is the regulation of the flue-gas temperature, the integrator for $T_{fg} = y_2$ is stopped.

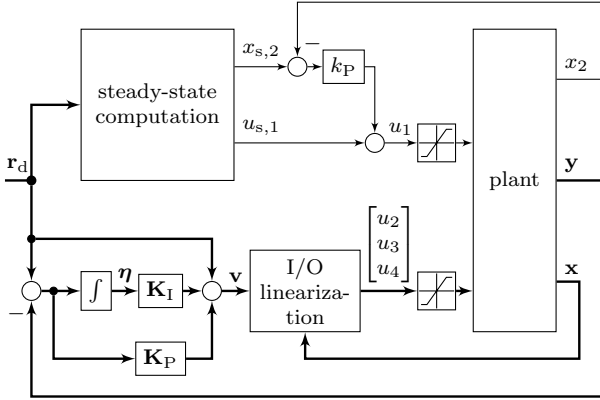


Figure 2: Overall structure of the existing control consisting of steady-state computation with fuel-feed controller and input-output linearization with PI-controllers; parameters of the latter are aggregated in diagonal matrices $\mathbf{K}_P = \text{diag}(K_{P,i})$ and $\mathbf{K}_I = \text{diag}(K_{I,i})$. Only the first three components of \mathbf{r}_d enter the PI-controllers; for clarity, this is not explicitly depicted.

3.6. Overall Control Structure

Figure 2 shows the overall control structure consisting of steady-state computation, fuel-feed controller, PI-controllers, input-output linearization, and the actuator saturations. The reconstruction of plant state \mathbf{x} and part of the disturbance vector \mathbf{d} by means of a Kalman filter, and the dependence of the control laws on \mathbf{d} is not depicted.

4. Reference Shaping

In this section the necessity of reference shaping is argued and the proposed reference shaping strategy is described.

4.1. Necessity of Reference Shaping

In the presented control strategy, reference values are used in two places: the steady-state computation and the PI-controllers followed by the input-output linearization. Consider first the steady-state computation. If the mass-flows corresponding to the steady-state inputs \mathbf{u}_s obtained from (14) exceed the limits (18), the desired steady state is not attainable. The steady state attained with the overall control concept will thus differ from the desired one, which may for example lead to a deviation of the air ratio λ_{fb} from its reference. Depending on this deviation and the actuator constraints, also other quantities, such as the feed temperature, may exhibit constant deviations as a consequence.

Also the input-output linearization suffers from problems when actuator saturations occur. If the mass-flows do not match those obtained from (11), the closed-loop dynamics will differ from the desired dynamics (10). In this case the PI-controllers may still eliminate steady-state control errors for all but those outputs where the anti-windup measure is active. Closed loop performance will

deteriorate, however, due to cross-couplings and nonlinearities being reintroduced. Depending on which actuator constraints are active, increased emissions or reduced efficiency could be the consequence. Furthermore, as it is shown in Seeber et al. (2014), windup effects are not completely eliminated, which leads to undesirable overshoots of certain controlled outputs such as the flue-gas temperature.

Appropriately modifying the references such that no actuator saturations occur avoids these problems, provided that the modification is reasonable from a process engineering point of view. Feeding these references to the PI-controllers additionally prevents integrator windup, which may in fact be interpreted as an instance of the conditioning technique proposed in Hanus et al. (1987). Using reference shaping instead of stopping the integrators thus reduces windup effects even further.

Distinct reference shaping filters are used for the two cases steady-state computation and PI-controllers. This way it is possible to (intermittently) change the references for the PI-controllers without necessarily changing the desired steady state. The same general strategy is applied to both cases; it is presented in the next section. The differences in applying this strategy to each case are discussed afterwards, in Section 5.

4.2. General Strategy

Motivated by (14) and (16), the basic strategy for modifying the reference values assumes the general relation $\mathbf{r} = \mathbf{g}(\mathbf{u})$ between m reference values \mathbf{r} and the control input vector \mathbf{u} , with the components of \mathbf{g} having the form

$$r_i = g_i(\mathbf{u}) = \frac{\mathbf{a}_i^T \mathbf{u} + b_i}{\mathbf{c}_i^T \mathbf{u} + d_i} \quad (19)$$

for $i = 1, \dots, m$. Depending on whether the steady-state references or the PI-controllers' references are considered, the coefficients of these relations are taken from either (14) or (16), respectively. As above, all denominators are assumed to be positive for physically meaningful values of \mathbf{u} .

Clearly, the references \mathbf{r} should be as close as possible to the desired references \mathbf{r}_d specified by the plant operator, while satisfying all actuator constraints with \mathbf{u} . This leads to an optimization problem, whose principal constraints are given by the actuator limitations and whose cost function may be chosen to quantify the relative desirability of different reference value deviations.² The following subsections discuss the structure of the constraints, the choice of the cost function and the solution of the resulting optimization problem.

²This strategy is similar to the model predictive control (MPC) technique, see e.g. Maciejowski (2002), which also uses optimization to deal with actuator limitations; it may in fact be viewed as a one-step MPC, as no predicted plant states or inputs are considered.

4.2.1. Structure of Constraints

Choosing the vector \mathbf{u} as the decision variables of the optimization problem, the structure of the constraints is investigated first. Using (7), the mass-flow limits can be represented as the following linear constraints:

$$\dot{\mathbf{m}}_{\min} \leq \mathbf{M}\mathbf{u} + \mathbf{n} \leq \dot{\mathbf{m}}_{\max} \quad (20a)$$

with

$$\mathbf{M} := \begin{bmatrix} 1 & 0 & 0 & 0 \\ 0 & 1 & 0 & 0 \\ 0 & -1 & 0 & 1 \\ 0 & 0 & 1 & 0 \end{bmatrix}, \quad \mathbf{n} := \begin{bmatrix} 0 \\ -C_3 \\ C_3 \\ 0 \end{bmatrix}. \quad (20b)$$

Additionally, certain constraints on the references may be prescribed. Consider for example the flue-gas oxygen content, which must stay above a given lower threshold *at all times*, or the power output (in the form of the feed temperature), which must not exceed the desired power output *in steady state*. Due to the structure of the function \mathbf{g} , such constraints may be written as linear inequality constraints on \mathbf{u} . For example, a lower bound

$$r_i \geq r_{\min,i} \quad (21)$$

on r_i can be rewritten, using relation (19) and the fact that the denominator is positive, as

$$\left(\mathbf{a}_i^T - \mathbf{c}_i^T r_{\min,i} \right) \mathbf{u} \geq d_i r_{\min,i} - b_i. \quad (22)$$

An upper bound may be handled analogously.

For the purpose of the following considerations, all these mass-flow and hard reference constraints are assumed to be aggregated in the linear inequality

$$\mathbf{P}_1 \mathbf{u} \geq \mathbf{w}_1 \quad (23)$$

with constant matrix \mathbf{P}_1 and vector \mathbf{w}_1 .

4.2.2. Choice of Cost Function

The choice of the cost function is less straightforward. On the one hand, it should reflect the wishes of the plant operator regarding control deviations during actuator saturations. On the other hand, the resulting optimization problem should ideally be a convex problem to be easily solvable. The seemingly obvious choice, a sum of squared errors, leads to a non-convex problem; finding the global minimum in this case is a non-trivial problem.

A strategy that leads to convex optimization problems while being reasonable from a practical point of view is now presented. It assumes that the references have different priorities, i.e. that a ranking exists, where keeping higher ranked references equal to their desired values is—loosely speaking—“infinitely” more important than doing so for those ranked beneath. This is indeed a valid assumption: for example, compared to upholding the desired feed temperature (and thus the power output), most other plant outputs are secondary as long as they do not violate

any hard constraints. This enables performing a *sequential optimization* of a series of cost functions, each weighting only the deviation of one reference. It will be shown that this way a series of convex problems is obtained.

For that purpose, the following non-negative cost functions are introduced

$$q_{i+}(\mathbf{u}) := \begin{cases} |g_i(\mathbf{u}) - r_{d,i}| & g_i(\mathbf{u}) - r_{d,i} \geq 0 \\ 0 & \text{otherwise,} \end{cases} \quad (24a)$$

$$q_{i-}(\mathbf{u}) := \begin{cases} 0 & g_i(\mathbf{u}) - r_{d,i} \geq 0 \\ |g_i(\mathbf{u}) - r_{d,i}| & \text{otherwise.} \end{cases} \quad (24b)$$

The functions q_{i+} and q_{i-} measure the upper and lower deviation, respectively, of the reference r_i in comparison to its desired value $r_{d,i}$. These $2m$ values q_j are indexed by the symbols

$$j \in \{1^+, 1^-, 2^+, 2^-, \dots, m^+, m^-\}. \quad (25)$$

They are minimized sequentially in an order $q_{j_1}, q_{j_2}, \dots, q_{j_{2m}}$ given in the form of a finite sequence denoted \mathcal{S} ,

$$\mathcal{S} := (j_1, j_2, \dots, j_{2m}), \quad (26)$$

by solving the (nonlinear) optimization problems

$$q_{j_k}^* := \min_{\mathbf{u}} q_{j_k}(\mathbf{u}) \quad (27a)$$

subject to

$$\mathbf{P}_1 \mathbf{u} \geq \mathbf{w}_1 \quad (27b)$$

$$q_{j_l}(\mathbf{u}) = q_{j_l}^* \quad \text{for } l < k \quad (27c)$$

for $k = 1, \dots, 2m$. During each optimization, the results of the previous optimizations are added in the form of the equality constraints (27c). This means that first the minimum $q_{j_1}^*$ of q_{j_1} subject to mass-flow and hard reference constraints (23) is determined, then q_{j_2} is minimized subject to these and the *additional* constraint $q_{j_1} = q_{j_1}^*$, and so on.

Before the solution of these problems is considered, the structure of the equality constraints should be highlighted. The equality constraint $q_{i\pm} = q_{i\pm}^*$ is, in the case $q_{i\pm}^* > 0$, equivalent to the equality constraint

$$g_i(\mathbf{u}) = r_{d,i} \pm q_{i\pm}^*, \quad (28)$$

i.e. when the deviation is known the corresponding reference value is fixed. In the case $q_{i\pm}^* = 0$ it is equivalent to the inequality constraint

$$\pm g_i(\mathbf{u}) \leq \pm r_{d,i}, \quad (29)$$

i.e. when the upper or lower deviation are zero, the reference must stay below or above the corresponding desired value, respectively. In both cases, multiplication with the denominator of $g_i(\mathbf{u})$ yields a linear equality or inequality constraint similar to (22).

4.2.3. Solution of Optimization Problems

The solution of the k -th optimization problem is now considered. For notational simplicity, all (linear) equality and inequality constraints (27b) and (27c) of this problem are assumed to be aggregated in the inequality

$$\mathbf{P}_k \mathbf{u} \geq \mathbf{w}_k \quad (30)$$

whose coefficients \mathbf{P}_k , \mathbf{w}_k depend on results $q_{j_1}^*, \dots, q_{j_{k-1}}^*$ of the previous optimizations, on the matrix \mathbf{P}_1 and on the vector \mathbf{w}_1 . It is further assumed that in this k -th step a lower deviation q_{i^-} is minimized, i.e. that $j_k = i^-$. The solution for an upper deviation q_{i^+} is completely analogous. A formulation of the optimization problem (27) is in this case

$$q_{j_k}^* = \min_{\mathbf{u}, q} q \quad (31a)$$

subject to

$$\mathbf{P}_k \mathbf{u} \geq \mathbf{w}_k \quad (31b)$$

$$\frac{\mathbf{a}_i^T \mathbf{u} + b_i}{\mathbf{c}_i^T \mathbf{u} + d_i} + q \geq r_{d,i} \quad (31c)$$

$$q \geq 0. \quad (31d)$$

The newly introduced optimization variable q is a non-negative upper bound of the considered deviation due to inequality constraints (31c) and (31d). Minimization of this upper bound yields the optimal upper deviation $q_{j_k}^*$ defined by (27). Due to the nature of the nonlinearity, this is a so-called linear-fractional optimization problem. Though non-convex, it can be transformed to a linear program by a clever change of variables due to Charnes and Cooper (1962). To that end, \mathbf{u} is replaced by new optimization variables defined as

$$\mathbf{z} := \mathbf{u}\sigma \quad (32)$$

with an additional *positive* optimization variable σ . This additional degree of freedom is used by adding the equality constraint

$$\sigma(\mathbf{c}_i^T \mathbf{u} + d_i) = 1 \quad (33)$$

which eliminates the denominator in (31c). One thus obtains the equivalent linear program

$$q_{j_k}^* = \min_{\mathbf{z}, q, \sigma} q \quad (34a)$$

subject to

$$\mathbf{P}_k \mathbf{z} - \mathbf{w}_k \sigma \geq \mathbf{0} \quad \sigma \geq 0 \quad (34b)$$

$$\mathbf{a}_i^T \mathbf{z} + b_i \sigma + q \geq r_{d,i} \quad q \geq 0 \quad (34c)$$

$$\mathbf{c}_i^T \mathbf{z} + d_i \sigma = 1 \quad (34d)$$

which can easily be solved by state-of-the-art techniques. Note that although $\sigma = 0$ satisfies $\sigma \geq 0$, it is excluded by the other constraints on \mathbf{z} and σ . This can be seen from (33): if $\sigma \rightarrow 0$, then \mathbf{u} tends to infinity, which is impossible due to the constraints (20) included in (34b).

The optimal solutions \mathbf{z}^* and σ^* for \mathbf{z} and σ of the final, i.e. the $2m$ -th, of these optimization problems yield the shaped input and reference values denoted by \mathbf{u}^* and \mathbf{r}^* , respectively:

$$\mathbf{u}^* = \frac{\mathbf{z}^*}{\sigma^*}, \quad \mathbf{r}^* = \mathbf{g}(\mathbf{u}^*). \quad (35)$$

5. Implementation Considerations

In this section the application of the previously discussed reference shaping strategy to both the steady-state computation and the PI-controllers is discussed.

5.1. Steady-State Computation

Consider the application of the strategy outlined in Section 4.2 to the steady-state computation. In this case, the function \mathbf{g} is given by \mathbf{g}_s from (14), and \mathbf{u}^* corresponds to the steady-state inputs \mathbf{u}_s . To account for the periodic disturbance present in the form of the varying fuel decomposition rate, a small modification of the optimization problems is required. This modification as well as the optimization sequence used and the reference constraints imposed are discussed subsequently.

5.1.1. Consideration of Periodic Disturbance

The periodic variations of the fuel decomposition factor α_{th} require special attention. As the control goal is to keep y_1 , y_2 and y_3 constant, the periodic variations of α_{th} require periodic variations of the plant inputs: From (3), (4a) and (5) one can see that constant outputs require constant mass-flows. Thus it is evident from (7) and (8) that $\alpha_{th} u_2$, u_3 and u_4 need to be constant when all other disturbances except α_{th} as well as x_1 and x_2 are constant. Given that the steady-state inputs \mathbf{u}_s are computed for $\alpha_{th} = 1$, the actual time-varying plant inputs in steady-state operation are given by

$$\mathbf{u}(t) = \mathbf{D}[\alpha_{th}(t)] \cdot \mathbf{u}_s \quad (36)$$

with the diagonal matrix $\mathbf{D}(\alpha_{th}) = \text{diag}(1, \alpha_{th}^{-1}, 1, 1)$.

The attainability of a certain steady state requires that not only the mean values \mathbf{u}_s , but also the actual time varying inputs $\mathbf{u}(t)$ satisfy the mass-flow limits. Due to convexity reasons, it is sufficient that the constraints be satisfied for both the minimal and the maximal value of α_{th} . These values are denoted $\alpha_{th, \min}$ and $\alpha_{th, \max}$, respectively, and are assumed to be known. For the purpose of applying the reference shaping strategy to the steady-state computation, the mass-flow constraints (20) are thus replaced by

$$\dot{\mathbf{m}}_{\min} \leq \mathbf{M}\mathbf{D}(\alpha_{th, \min})\mathbf{u} + \mathbf{n} \leq \dot{\mathbf{m}}_{\max}, \quad (37a)$$

$$\dot{\mathbf{m}}_{\min} \leq \mathbf{M}\mathbf{D}(\alpha_{th, \max})\mathbf{u} + \mathbf{n} \leq \dot{\mathbf{m}}_{\max}. \quad (37b)$$

5.1.2. Optimization Sequence and Reference Constraints

Permanently exceeding the prescribed feed temperature $r_{d,3}$ or dropping below the prescribed flue-gas oxygen content $r_{d,1}$ must be avoided at all costs. The hard reference constraints

$$r_1 \geq r_{d,1}, \quad r_3 \leq r_{d,3} \quad (38)$$

are thus added to reflect these wishes. Additionally, the flue-gas temperature r_2 and the air ratio r_4 are constrained by reasonable lower and (in the case of r_2) upper bounds that prevent any damage to the plant and ensure its safe operation, i.e. constraints of the form

$$r_{2,\min} \leq r_2 \leq r_{2,\max}, \quad r_{4,\min} \leq r_4 \quad (39)$$

are imposed.

Assuming the combustion of conventional wood chips, the steady-state optimization sequence \mathcal{S}_s is chosen as

$$\mathcal{S}_s = (2^-, 3^-, 4^-, 2^+, 1^+, 4^+). \quad (40)$$

This sequence is shorter than $2m = 8$ as assumed in Section 4.2. This is due to the hard reference constraints on r_1 and r_3 . The complete sequence can be thought of as being

$$\mathcal{S}_s = (1^-, 3^+, 2^-, 3^-, 4^-, 2^+, 1^+, 4^+) \quad (41)$$

with the first two optimizations yielding $q_{1-}^* = q_{3+}^* = 0$ due to (38). Though avoiding any deviation of the feed temperature is of highest priority, the lower deviation q_{2-} of the flue-gas temperature is minimized first. This is due to the fact that otherwise the flue-gas recirculation may be used to (temporarily) increase the power output by using the energy stored in the refractory lining, whose temperature is given by the disturbance T_{r1} . As the steady-state computation assumes T_{r1} to be constant, this seems a viable option from the perspective of the mathematical model used. From a physical point of view it is clear, however, that nothing can be gained by this as it leads to a reduced flue-gas temperature and as a consequence the temperature T_{r1} will eventually drop.

The deviation q_{3-} of the feed temperature r_3 is thus minimized after q_{2-} . Next, the lower deviation of the reference r_4 for the air ratio in the fuel bed is chosen as small as possible. Finally, the upper deviations of flue-gas temperature r_2 , oxygen content r_1 and air ratio r_4 are minimized. A lower oxygen content r_1 is preferred to a smaller deviation of the air ratio r_4 , because the former leads to increased plant efficiency and deviations of the latter do not significantly deteriorate combustion conditions for wood chips. In general, the air ratio in the fuel bed influences emissions as well as the ash melting behavior, though; for other furnaces or fuels, different sequences may thus be chosen.

5.2. PI-Controllers

The application of the reference shaping strategy to the PI-controllers is discussed next. In this case, the function \mathbf{g} is given by \mathbf{g}_p from (16), and the components of

\mathbf{u}^* correspond to the inputs u_2 , u_3 and u_4 applied to the plant. First, the prevention of integrator windup is discussed, and afterwards the optimization sequence and the reference constraints used in this case are shown.

5.2.1. Prevention of Integrator Windup

The reference shaping may be used to prevent integrator windup in a simple yet effective way. This is due to the fact that, by design, applying the shaped references \mathbf{r}^* to the controller leads to the plant inputs \mathbf{u}^* , which satisfy the constraints. Applying \mathbf{r}^* , in particular, to the PI-controllers' integrators thus prevents integrator windup, because the closed loop responds to the shaped references as if no actuator constraints were present at all. Thus, (15a) is replaced with

$$\frac{d\eta_i}{dt} = r_i^* - y_i \quad i = 1, 2, 3, \quad (42)$$

i.e. the shaped references \mathbf{r}^* are used not only for the calculation of the plant inputs but also for updating the integrator states.

This may be interpreted as an instance of the *conditioning technique* introduced by Hanus et al. (1987). There, the idea is to compute realizable references, which, when applied to the controller, lead to plant inputs that satisfy the constraints. Feeding these modified references to the dynamic part of the controller prevents any controller windup. Here, the shaped references \mathbf{r}^* given in (35) constitute such realizable references, with the only difference to the original conditioning technique being the way they are computed.

5.2.2. Optimization Sequence and Reference Constraints

It is a reasonable requirement that the reference shaping used for the PI-controllers in steady-state operation should match the results of the steady-state reference shaping. More precisely, at least when the air ratio $y_4 = r_4^*$ and the fuel decomposition factor $\alpha_{th} = 1$, the reference shaping for the PI-controllers should yield the same results as for the steady-state case. Otherwise, the computed steady state may not be attained due to the PI-controller references being modified in a different way than the steady-state references. This may be ensured by the consistency of optimization sequence and constraints: They must be the same, with the exceptions that in the PI-controller case, the fourth reference value is not present and that the reference constraints may be relaxed compared to the steady-state case. No additional (more stringent) constraints or reorderings of the optimization sequence may be imposed, though, unless the consistency of reference shaping results can be ensured by other means.

Because temporarily exceeding the desired feed temperature (as opposed to permanently doing so) is tolerable, only the first reference constraint from (38), i.e.

$$r_1 \geq r_{d,1} \quad (43)$$

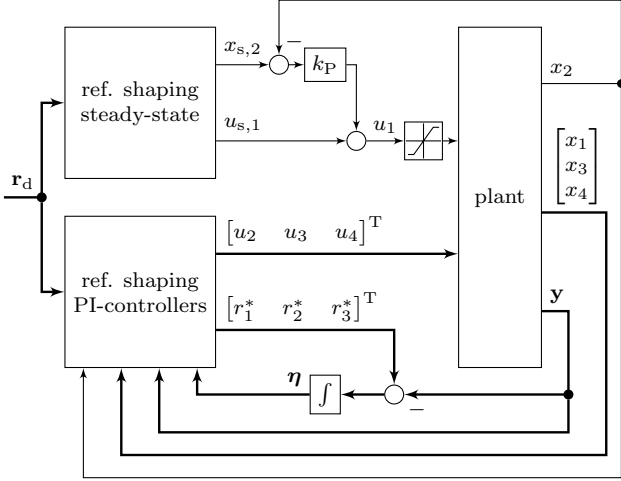


Figure 3: Overall control structure with reference shaping applied to both the steady-state and the PI-controller references

is used. The PI-controller optimization sequence \mathcal{S}_p is consequently chosen as

$$\mathcal{S}_p = (3^+, 2^-, 3^-, 2^+, 1^+). \quad (44)$$

One can see that the order is the same as in (40) apart from 4^+ and 4^- being dropped, and 3^+ being added in first place to account for the removed reference constraint on r_3 .

5.3. Overall Structure

The overall structure of the control strategy with reference shaping applied is shown in Figure 3: The reference shaping for the steady state yields the steady-state input $u_{s,1}$ and the fuel mass $x_{s,2}$ required in steady state, the latter being obtained using (13). These are applied to the fuel-feed controller, whose output u_1 is limited to the available actuator range by a saturation function; in steady state, u_1 stays within the limits. The reference shaping for the PI-controllers depends on the plant and integrator states \mathbf{x} and $\boldsymbol{\eta}$, as these are parameters of the function \mathbf{g}_p . It generates plant inputs u_2 , u_3 and u_4 that do not cause actuator saturation and are thus applied to the plant directly. The corresponding shaped (realizable) references are used to compute the control error that drives the PI-controllers' integrators. All control laws that are not visible here, i.e. the input-output linearization and the output equation of the PI-controllers, are realized by using \mathbf{g}_p as the non-linear function for the reference shaping strategy. Not shown explicitly are the dependence of both reference shaping strategies on the disturbance vector \mathbf{d} , and the Kalman filter reconstructing the state vector \mathbf{x} and part of the disturbance vector \mathbf{d} .

5.4. Estimation of Mass-flow Limits

To apply the described technique, the mass-flow limits need to be known. The mass-flows, however, are generated by fans and controlled by throttle valves. Limits thus

are known only for these actuators, but not for the mass-flows themselves. Their limits have to be estimated (or at least detected) dynamically from actuator signals and corresponding measured mass-flows. A straightforward approach is to store the previously attained maximal and minimal values for each mass-flow, and use those as limits in the optimization. When a mathematical model relating fan speeds and valve positions to mass-flows is available, more accurate limits can be obtained.

This subsection describes a simple strategy to do this based on the model for the secondary air supply proposed in Schörghuber et al. (2014). It can straightforwardly be applied to other similar (sufficiently accurate) mathematical models. The mass-flow of secondary air predicted by the model $\dot{m}_{sa,mdl}$ is given by the static nonlinear function

$$\dot{m}_{sa,mdl} = s(\varphi, \omega) := c_v(\varphi) \cdot \sqrt{c_f \omega^2 - \Delta p} \quad (45)$$

of valve position φ and fan speed ω . Therein $c_v(\varphi)$ is the monotonous valve characteristic, c_f is a constant model parameter and Δp is the measureable pressure difference across both valve and fan. The last quantity acts as a disturbance on the model, but is kept approximately constant by the flue-gas fan.

Given the actuator limitations

$$\varphi_{\min} \leq \varphi \leq \varphi_{\max}, \quad \omega_{\min} \leq \omega \leq \omega_{\max} \quad (46)$$

one may observe that s takes its minimal and maximal values for $\varphi_{\min}, \omega_{\min}$ and $\varphi_{\max}, \omega_{\max}$, respectively. Estimates $\dot{m}_{sa,\min}$ and $\dot{m}_{sa,\max}$ for the minimal and maximal mass-flows, respectively, can thus be computed from measurements as

$$\dot{m}_{sa,\min} = \frac{s(\varphi_{\min}, \omega_{\min})}{s(\varphi, \omega)} \dot{m}_{sa}, \quad (47a)$$

$$\dot{m}_{sa,\max} = \frac{s(\varphi_{\max}, \omega_{\max})}{s(\varphi, \omega)} \dot{m}_{sa}. \quad (47b)$$

For this approach to work, the mass-flow controller prescribing φ and ω must ensure either that ω and φ tend to their upper or lower limits, or that the mass-flow asymptotically matches its reference. Otherwise, the computed mass-flow limits may not be attainable in practice due to the controller not using the full actuators' operating ranges to steer the control error to zero.

The described strategy is used for all mass-flows except the fuel-feed \dot{m}_{ff} , which is not measured but instead computed from the screw conveyor's speed using a static model. Therefore, the maxima and minima predicted by the model are in that case used directly, without a multiplicative correction as in (47).

6. Experimental Results

The presented reference shaping strategy was implemented on a medium-scale biomass grate boiler with 180 kW

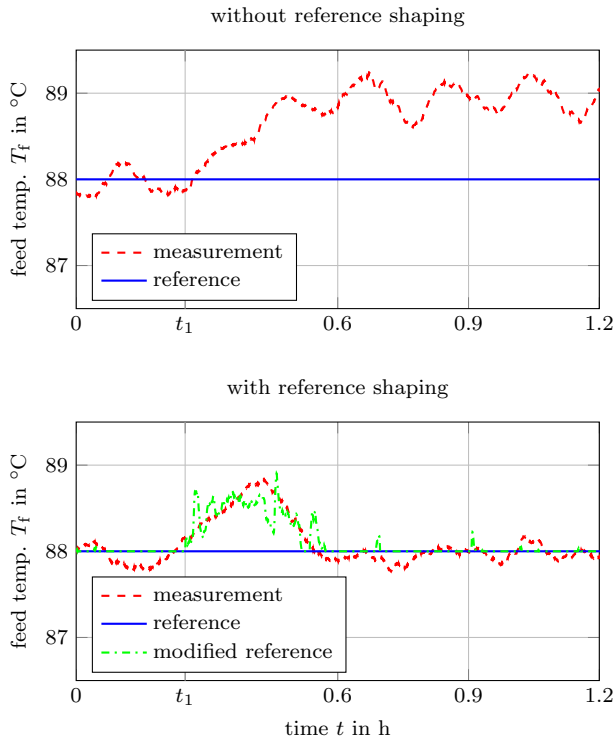


Figure 4: Measured feed temperature T_f as well as its reference while imposing the limit $\dot{m}_{pa} \geq 55 \text{ kg/h}$ on the primary air starting at time $t_1 = 0.25 \text{ h}$

nominal capacity operating as described in Section 2. Several experiments using this control structure were conducted and are compared to results obtained with the control strategy as described in Seeber et al. (2014) without *any*³ reference shaping, but with otherwise identical controller parameters and mass-flow constraints. The following subsections A, B, and C show the results of three such experiments: an artificial lower limit on the primary air during steady-state operation at 60 kW, a subsequent load change from 60 kW to 180 kW, and an artificial upper limit on the primary air during steady-state operation at 180 kW. The artificial limitations are introduced for demonstration purposes, but are nonetheless representative, as for research purposes the considered plant is equipped with more powerful actuators than comparable industrial furnaces. Also the sudden changes of limitations can occur in practice due to actuator failures. Apart from the artificial limitations, flue-gas recirculation and secondary air mass-flows were at their lower limits during operation at 60 kW.

³As noted in the introduction, the model-based control strategy usually requires reference modifications for its successful use, with expert rules typically being used for that purpose. Due to their plant-dependent nature, and to clearly demonstrate the reference shaping filters' operation, no such strategies were used in the course of the experiments presented here.

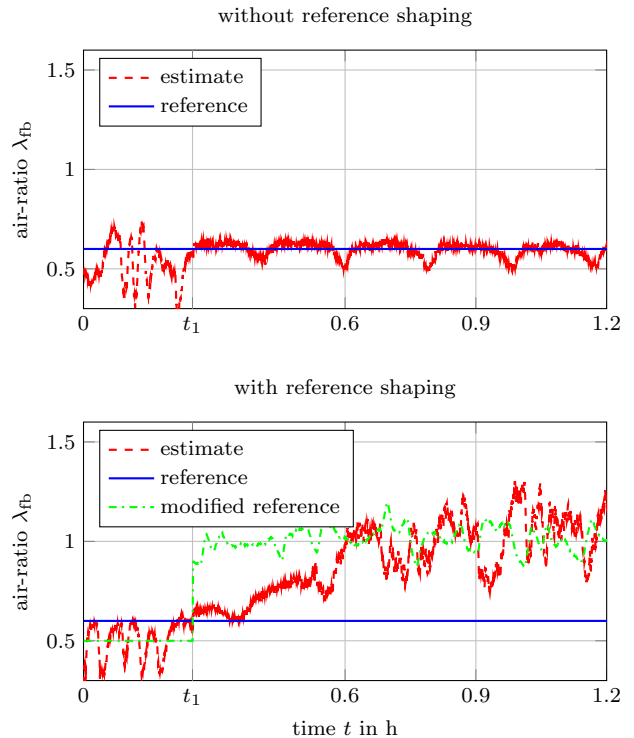


Figure 5: Estimated air ratio in the fuel-bed λ_{fb} as well as its reference while imposing the limit $\dot{m}_{pa} \geq 55 \text{ kg/h}$ on the primary air starting at time $t_1 = 0.25 \text{ h}$

6.1. Lower Limit of Primary Air

During steady-state operation with a power output of 60 kW the lower limit for the primary air mass-flow \dot{m}_{pa} was artificially set to 55 kg/h. Figure 4 shows the controlled feed temperature, i.e. y_3 , with and without the reference shaping strategy being used.

Without reference shaping, the integrator of the PI-controller responsible for this output is stopped and a control deviation results. From a process point of view this corresponds to a power output that is higher than requested, which is caused by too much fuel being fed into the plant. With the return temperature T_r being kept constant, this is not a critical problem for the considered *experimental* plant. In a more realistic setting, however, this surplus power would go unused and thus would lead to a steadily increasing temperature of the circulating water. This would have to be detected and responded to by forcibly reducing or switching off the fuel feed.

When reference shaping is used, this feed temperature deviation is only temporary. The reason for this is visible in Figure 5, which depicts the corresponding air ratio in the fuel bed λ_{fb} . As this quantity can not be measured directly, an estimate obtained using the Kalman filter employed by the control strategy is shown. It can be seen that the reference for the air ratio is increased, which leads to more primary air being required for the same power output. As a consequence, the primary air mass-flow \dot{m}_{pa} eventually increases beyond the lower limit, and power

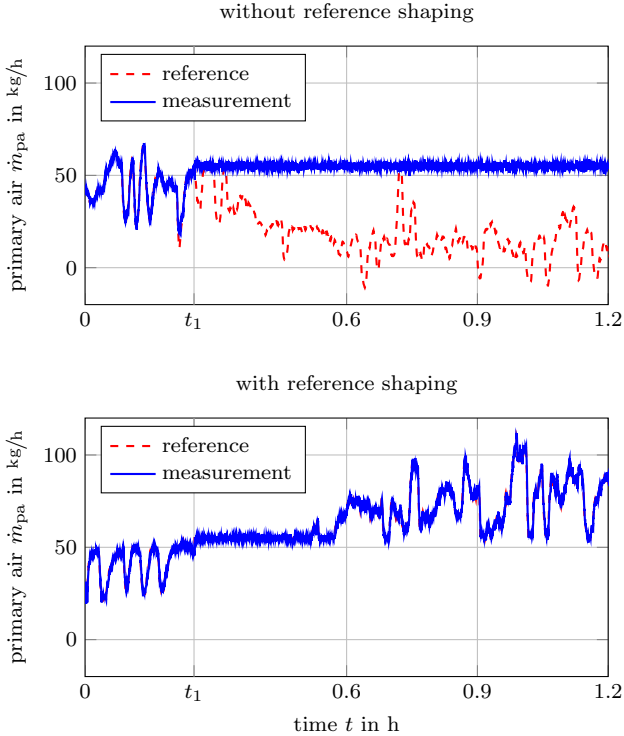


Figure 6: Measured primary air mass-flow \dot{m}_{pa} as well as its reference as prescribed by the input-output linearization while imposing the limit $\dot{m}_{pa} \geq 55$ kg/h on the primary air starting at time $t_1 = 0.25$ h

output is restored to its desired value. This can also be seen in Figure 6, which shows desired and measured primary air mass-flows. It is obvious that these two signals (almost) coincide when the reference shaping strategy is used, as in this case only mass-flows above the prescribed limit are requested.

Figure 5 furthermore shows that the reference for λ_{fb} is also modified before the artificial primary-air limit becomes active. This is due to the steady-state secondary air mass-flow being at its lower limit. In order to minimize the excess oxygen content in the flue-gas the air ratio λ_{fb} is reduced to its lower bound, for which the value 0.5 was prescribed in this experiment. This leads to the minimal amount of primary air being used and thus maximizes the plant's efficiency.

6.2. Load Change

Following the experiment shown in the previous section, a rapid load change was performed by a stepwise change of the water mass-flow \dot{m}_w while keeping the desired feed temperature constant. This way the boiler load was increased from 60 kW to the nominal load of 180 kW. Figure 7 shows the secondary air mass-flow \dot{m}_{sa} along with its estimated upper and lower limits. For demonstration purposes, the reference shaping strategy is not active; the depiction of the reference value thus permits to identify time intervals where actuator saturations occur. One can see that the lower limit is accurately reconstructed, with

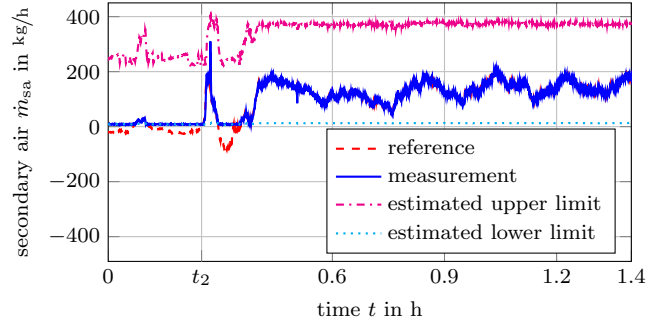


Figure 7: Measured secondary-air mass flow \dot{m}_{sa} , its reference as prescribed by the input-output linearization and the estimates for its limits during a load change from 60 kW to 180 kW starting at time $t_2 = 0.25$ h (without reference shaping)

only a slight deviation after the load change. The upper limit, though, only becomes reliable once the air mass-flow increases and shows a significant deviation while \dot{m}_{sa} is at its lower limit. As the limit is not used in the latter case, this does not influence the results shown here. Nonetheless, for a more reliable reconstruction the estimation strategy may be changed in the following way: use relations (47a) or (47b) only when φ and ω are close to the minima or maxima, respectively, and keep the estimates constant otherwise.

Figure 8 shows the controlled flue-gas temperature T_{fg} , i.e. y_2 , with and without using the reference shaping strategy. Furthermore, the output of the corresponding PI-controller is depicted in each case.

During operation at 60 kW the flue-gas recirculation is at its lower limit. Without reference shaping, the integrator of the PI-controller for y_2 is thus stopped, leading to a nonvanishing control deviation. Despite this measure, windup of the PI-controller output can be observed, leading to a significant overshoot in response to the load change. The integrator value at the start of this experiment is far from atypical: It is the consequence of a previous load change (not shown here) where power output was gradually decreased from 180 kW to 60 kW over the course of 15 minutes. During the artificial limitation of the primary air mass-flow described before this value did not change, as the flue-gas recirculation stayed at its lower limit all the time.

When the reference shaping strategy is employed, the overshoot is significantly reduced. The output on average matches the modified reference, such that no windup occurs. As a consequence the thermal stress on the refractory lining caused by higher temperatures and fast temperature changes is reduced, which can significantly increase the lifetime of the refractory lining.

It is apparent that at the start of the experiment the flue-gas temperature is lower when reference shaping is used than otherwise. This is a consequence of tracking the desired power more accurately in the course of the previous experiment.

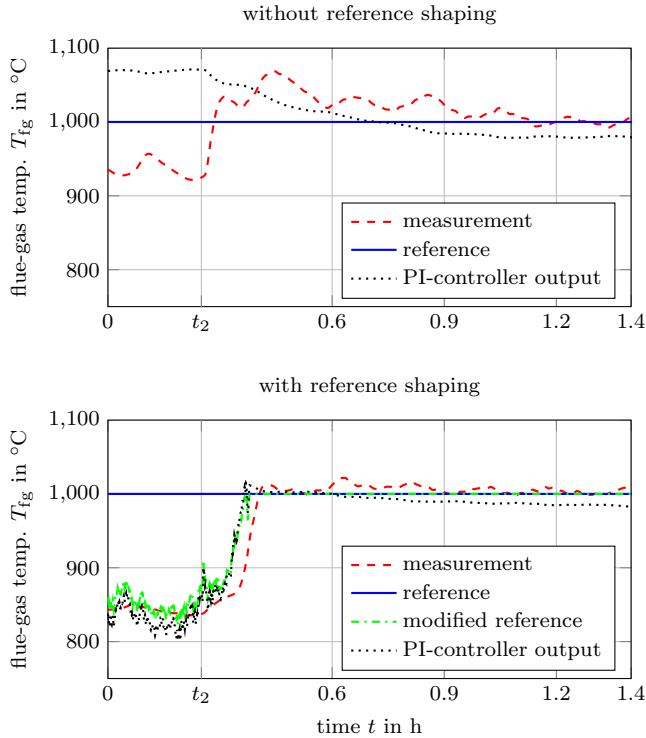


Figure 8: Measured flue-gas temperature T_{fg} , its reference and corresponding PI-controller output during a load change from 60 kW to 180 kW starting at time $t_2 = 0.25$ h

6.3. Upper Limit of Primary Air

During steady-state operation with a power output of 180 kW, which corresponds to full boiler load, an artificial upper limit on the primary air of 140 kg/h was introduced. Due to the time-varying fuel decomposition factor, this limit (initially) was active approximately one third of the time. Similar to the previously discussed artificial lower limit, a permanent deviation of the feed temperature resulted without reference shaping which was overcome by decreasing the reference for the air ratio λ_{fb} . As these results are similar to those already discussed for the lower limit of the primary air, they are not shown here. Instead, the flue-gas temperature T_{fg} shown in Figure 9 is investigated. Here, larger variations are visible when no reference shaping is used. This is due to nonlinear couplings being reintroduced. With reference shaping in place, these variations and as a consequence also the thermal stress on the refractory lining are reduced. A small control deviation is visible even in this case; this can be explained by differences between the mathematical model and the true plant behavior.

Figure 10 depicts the carbon monoxide emissions obtained from a flue-gas analyser. Without the reference shaping strategy, these emissions are unnecessarily large. This increase in emissions is caused by the increased variations of T_{fg} together with sub-optimal flow conditions specific to the considered furnace: While the difference in the variations' magnitude in Figure 9 may at first seem

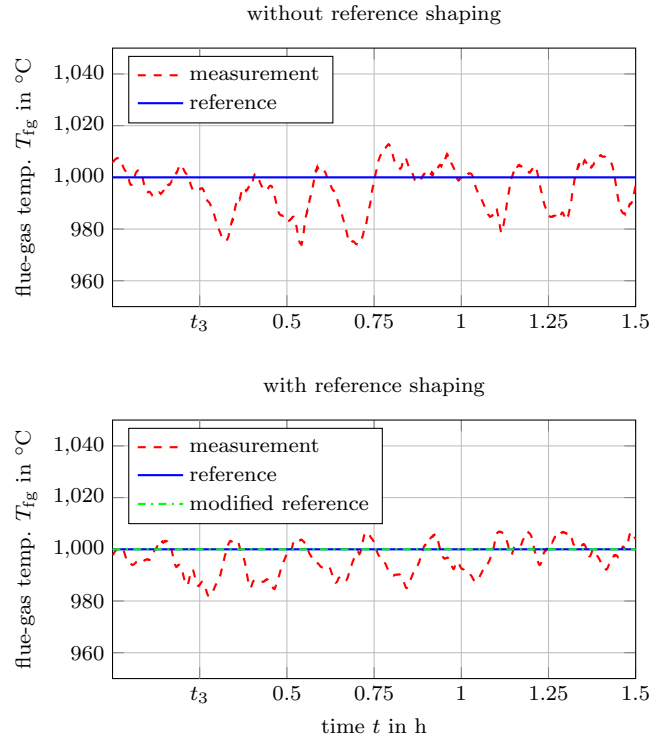


Figure 9: Measured flue-gas temperature T_{fg} as well as its reference while imposing the limit $\dot{m}_{pa} \leq 140$ kg/h on the primary air starting at time $t_3 = 0.25$ h

small, one has to take the dynamic behavior of the temperature sensor into account. For very fast changes the first (or even the second) time derivative is a more accurate indicator for the true flue-gas temperature, see Bauer et al. (2007). Steep downward slopes of T_{fg} thus indicate a much lower flue-gas temperature, and can indeed be seen to coincide with the spikes in carbon monoxide emissions. Considering the extent of the increase in carbon monoxide emissions, this still has to go along with sub-optimal flow conditions. Even if this coincidence is specific to the plant and the operation conditions considered here, the result is still representative, however: The exact characteristic of the nonlinear coupling's effect on the increase in temperature variations will always depend on the specific plant's parameters and actuator limits. In all cases the increased temperature variations will abet higher carbon monoxide emissions as well as increase the thermal stress for the refractory lining.

7. Conclusion

The key features of the presented reference shaping strategy are its efficient implementation in the form of linear programs, its straightforward tuning according to the requirements of the plant operator, and the resulting performance improvements in case of actuator saturations.

Despite the nonlinear plant, the reference shaping strategy may be implemented in the form of a sequence of linear

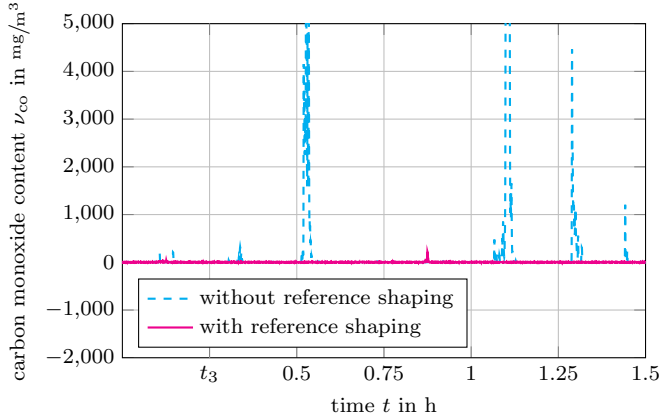


Figure 10: Carbon monoxide emissions per standard cubic meter of dry flue-gas while imposing the limit $\dot{m}_{pa} \leq 140 \text{ kg/h}$ on the primary air starting at time $t_3 = 0.25 \text{ h}$; their mean values are 3.89 mg/m^3 and 133.89 mg/m^3 with and without reference shaping, respectively.

programs. These programs are comparatively small, with five decision variables and typically less than twenty constraints. This enables the efficient and reliable execution of the strategy in real time.

The tuning is achieved by selecting a sequence of control goals, which are optimized sequentially. Their relative priority may be chosen according to requirements from a process engineering point of view, such as emissions and ash melting behavior of the fuel. One such sequence, which is suitable for a representative medium-scale biomass grate boiler, was provided and its use was demonstrated in the course of experiments.

The application of the presented reference shaping strategy leads to several improvements that were demonstrated experimentally. Most importantly, permanent deviations of the most crucial plant outputs are prevented to the greatest extent possible. During limitation of the primary air, for example, a permanent surplus in power output was shown to be avoided by adjusting the air ratio in the fuel bed. The technique furthermore prevents integrator windup in an effective way. During a load change, for instance, a significant overshoot of the flue-gas temperature caused by windup was eliminated almost completely, significantly reducing the thermal stress on the furnace refractory lining. In the presence of actuator limitations, the reference shaping additionally improved decoupling of outputs corresponding to unmodified references. This was exemplarily shown in the form of reduced flue-gas temperature variations when the primary air is limited; on the considered plant this in turn eliminated spikes in carbon monoxid emissions occurring otherwise.

It should be highlighted that the strategy, due to its systematic nature, can deal in an optimal way also with arbitrary other combinations of actuator limitations that are not demonstrated here. This permits uninterrupted plant operation even when actuators fail or, in the case of multiple actuators contributing to the same air mass-

flow, are partly disabled for maintenance reasons. In an industrial setting this can be an important asset, adding to the demonstrated improvements. In the future, it is therefore planned to implement this strategy on an industrial biomass grate boiler for the purpose of long-term validation. Furthermore, it may also be investigated whether using different anti-windup concepts instead of reference shaping also yield satisfactory plant behavior in the case of actuator saturations with reduced computational complexity.

Acknowledgment

The authors would like to thank Daniel Muschick, for numerous remarks and suggestions that have significantly improved this contribution, and Christoph Schörghuber, for countless discussions and useful comments regarding this work as well as the control of biomass grate boilers in general.

List of Symbols

symbol	description
α_{th}	fuel decomposition factor
λ_{fb}	air-ratio in the fuel bed
m_f	dry fuel mass in the fuel bed
\dot{m}_{fa}	mass-flow of false air
\dot{m}_{ff}	mass-flow of dry fuel
\dot{m}_{fg}	mass-flow of flue-gas
\dot{m}_{pa}	mass-flow of primary air
\dot{m}_{rf}	mass-flow of recirculated flue gas
\dot{m}_{sa}	mass-flow of secondary air
\dot{m}_{thd}	mass-flow of thermally decomposed dry fuel
m_w	water mass in the fuel bed
\dot{m}_w	water mass-flow through heat exchanger
\dot{m}_{wev}	mass-flow of evaporated water
ν_{ox}	flue-gas oxygen content
T_f	feed temperature
T_{fg}	flue-gas temperature
T_r	return temperature
T_{r1}	temperature of refractory lining
t_{df}	time delay of the fuel feed
t_{dr}	time delay of the return temperature
w_f	fuel water content (based on dry fuel mass)

References

References

Åström, K.J., Rundqwist, L., 1989. Integrator windup and how to avoid it, in: American Control Conference (ACC), IEEE. pp. 1693–1698.

- Bauer, R., Göllles, M., Brunner, T., Dourdoumas, N., Obernberger, I., 2007. What is really measured by temperature sensors in a biomass furnace? at – *Automatisierungstechnik* 55, 600–607. (in German).
- Bauer, R., Göllles, M., Brunner, T., Dourdoumas, N., Obernberger, I., 2008. Dynamic modelling of the heat transfer in a gas tube heat exchanger. at – *Automatisierungstechnik* 56, 513–520. (in German).
- Bauer, R., Göllles, M., Brunner, T., Dourdoumas, N., Obernberger, I., 2010. Modelling of grate combustion in a medium scale biomass furnace for control purposes. *Biomass and Bioenergy* 34, 417–427.
- Bemporad, A., 1998. Reference governor for constrained nonlinear systems. *IEEE Transactions on Automatic Control* 43, 415–419.
- Bemporad, A., Casavola, A., Mosca, E., 1997. Nonlinear control of constrained linear systems via predictive reference management. *IEEE Transactions on Automatic Control* 42, 340–349.
- Berger, A., Gutman, P.O., 2016. A new view of anti-windup design for uncertain linear systems in the frequency domain. *International Journal of Robust and Nonlinear Control* 26, 2116–2135.
- Charnes, A., Cooper, W.W., 1962. Programming with linear fractional functionals. *Naval Research Logistics Quarterly* 9, 181–186.
- Daoutidis, P., Kravaris, C., 1994. Dynamic output feedback control of minimum-phase multivariable nonlinear processes. *Chemical Engineering Science* 49, 433–447.
- De Lasa, M., Hertzmann, A., 2009. Prioritized optimization for task-space control, in: *IEEE/RSJ International Conference on Intelligent Robots and Systems*, pp. 5755–5762.
- Falkinger, M., Schell, S., Müller, J., Wilkens, J.J., 2012. Prioritized optimization in intensity modulated proton therapy. *Zeitschrift für Medizinische Physik* 22, 21–28. doi:10.1016/j.zemedi.2011.05.004.
- Garone, E., Di Cairano, S., Kolmanovsky, I., 2017. Reference and command governors for systems with constraints: A survey on theory and applications. *Automatica* 75, 306–328.
- Gilbert, E.G., Kolmanovsky, I., Tan, K.T., 1994. Nonlinear control of discrete-time linear systems with state and control constraints: A reference governor with global convergence properties, in: *33rd IEEE Conference on Decision and Control (CDC)*, pp. 144–149.
- Gilbert, E.G., Tan, K.T., 1991. Linear systems with state and control constraints: The theory and application of maximal output admissible sets. *IEEE Transactions on Automatic Control* 36, 1008–1020.
- Göllles, M., Bauer, R., Brunner, T., Dourdoumas, N., Obernberger, I., 2011. Model based control of a biomass grate furnace, in: *European Conference on Industrial Furnaces and Boilers*.
- Göllles, M., Reiter, S., Brunner, T., Dourdoumas, N., Obernberger, I., 2014. Model based control of a small-scale biomass boiler. *Control Engineering Practice* 22, 94–102.
- Hanus, R., Kinnaert, M., Henrotte, J.L., 1987. Conditioning technique, a general anti-windup and bumpless transfer method. *Automatica* 23, 729–739.
- Herrmann, G., Menon, P.P., Turner, M.C., Bates, D.G., Postlethwaite, I., 2010. Anti-windup synthesis for nonlinear dynamic inversion control schemes. *International Journal of Robust and Nonlinear Control* 20, 1465–1482.
- Hippe, P., 2006. *Windup in control: its effects and their prevention*. Springer.
- Isidori, A., 1995. *Nonlinear Control Systems*. Springer.
- Kalabić, U., Chitalia, Y., Buckland, J., Kolmanovsky, I., 2013. Prioritization schemes for reference and command governors, in: *European Control Conference (ECC)*, IEEE. pp. 2734–2739.
- Kalabić, U., Kolmanovsky, I., Gilbert, E., 2011. Reference governors for linear systems with nonlinear constraints, in: *50th IEEE Conference on Decision and Control and European Control Conference (CDC-ECC)*, IEEE. pp. 2680–2686.
- Kaltschmitt, M., Hartmann, H., Hofbauer, H. (Eds.), 2016. *Energie aus Biomasse – Grundlagen, Techniken und Verfahren*. 3rd ed., Springer. (in German).
- Kapasouris, P., Athans, M., Stein, G., 1988. Design of feedback control systems for stable plants with saturating actuators, in: *27th IEEE Conference on Decision and Control (CDC)*, IEEE. pp. 469–479.
- Kendi, T.A., Doyle III, F.J., 1997. An anti-windup scheme for multivariable nonlinear systems. *Journal of Process Control* 7, 329–343.
- Kolmanovsky, I., Gilbert, E.G., 1998. Theory and computation of disturbance invariant sets for discrete-time linear systems. *Mathematical Problems in Engineering* 4, 317–367.
- Kortela, J., Jämsä-Jounela, S.L., 2012. Model predictive control for biopower combined heat and power (chp) plant, in: *11th International Symposium on Process Systems Engineering*, Elsevier. pp. 435–439.
- Kothare, M.V., Campo, P.J., Morari, M., Nett, C.N., 1994. A unified framework for the study of anti-windup designs. *Automatica* 30, 1869–1883.
- van Loo, S., Koppejan, J. (Eds.), 2008. *The Handbook of Biomass Combustion and Co-Firing*. Earthscan.
- Maciejowski, J.M., 2002. *Predictive Control with Constraints*. Pearson Education.
- Paces, N., Voigt, A., Jakubek, S., Schirrer, A., Kozek, M., 2011. Combined control of combustion load and combustion position in a moving grate biomass furnace, in: *19th Mediterranean Conference on Control and Automation*, pp. 1447–1452.
- Plaček, V., Šulc, B., Vrána, S., Hrdlička, J., Pitell, J., 2011. Investigation in control of small-scale biomass boilers, in: *12th International Carpathian Control Conference (ICCC)*, IEEE. pp. 308–311.
- Schörghuber, C., Göllles, M., Dourdoumas, N., Obernberger, I., 2014. Model based control of the secondary air massflow of biomass furnaces. at – *Automatisierungstechnik* 62, 487–499. (in German).
- Schörghuber, C., Reichhartinger, M., Horn, M., Göllles, M., Seeber, R., 2015. Control of a biomass-furnace based on input-output-linearization, in: *2015 European Control Conference (ECC)*, IEEE. pp. 3508–3513.
- Seeber, R., Göllles, M., Brunner, T., Dourdoumas, N., Obernberger, I., 2014. Improvement of a model based control strategy for biomass furnaces. at – *Automatisierungstechnik* 62, 891–902. (in German).
- Gomes da Silva Jr., J., Oliveira, M., Coutinho, D., Tarbouriech, S., 2014. Static anti-windup design for a class of nonlinear systems. *International Journal of Robust and Nonlinear Control* 24, 793–810.
- Vahidi, A., Kolmanovsky, I., Stefanopoulou, A., 2007. Constraint handling in a fuel cell system: A fast reference governor approach. *IEEE Transactions on Control Systems Technology* 15, 86–98.
- Zemann, C., Heinrichsberger, O., Göllles, M., Brunner, T., Dourdoumas, N., Obernberger, I., 2014. Application of a model based control strategy at a fixed bed biomass district heating plant, in: *Proceedings of the 22nd European Biomass Conference and Exhibition, Hamburg, Germany*. pp. 1698–1705. doi:10.5071/22ndEUBCE2014-IBV.4.18.